Electronic Supplementary Material (ESI) for Physical Chemistry Chemical Physics.

Electronic Supplementary Information for:

Experimental and Theoretical Studies on Thymine Photodimerization Mediated by Oxidatively Generated DNA Lesions and Epigenetic Intermediates

Mauricio Lineros-Rosa,[a] Antonio Francés-Monerris,[b,c] Antonio Monari,*[,b] Miguel Angel Miranda,*[,a] and Virginie Lhiaubet-Vallet*[,a]

[a]*Instituto Universitario Mixto de Tecnologia Química UPV-CSIC, Universitat Politècnica de València, Avda de los Naranjos s/n, 46022 Valencia, Spain.*

[b]*Université de Lorraine and CNRS, LPCT UMR 7019, F-54000 Nancy, France.*

[c]*Departament de Química Física, Universitat de València, 46100 Burjassot, Spain*

E-mail: *A.M.: antonio.monari@univ-lorraine.fr, M.A.M.: mmiranda@qim.upv.es, V.L.-V.: lvirgini@itq.upv.es

Table of contents

Materials, methods, and computational details

Chemicals

The chemicals 5-formyluracil, o,o'-bis(trimethylsilyl)thymine, 1,3-dibromopropane, sodium hydride, iodomethane, trifluoroacetic acid and anhydrous N,N-dimethylformamide were purchased from Sigma-Aldrich. 5-Formylcytosine was purchased from Toronto Research Chemicals. Ethanol, methanol, acetonitrile, dichloromethane and acetone of HPLC grade were purchased from Scharlau, whereas water was purified using Milli-Q system (IQ 7000, Merck). Phosphate buffered saline (PBS) tablets were purchased from Sigma Aldrich and used to prepare PBS solutions in Milli-Q water at pH 7.4 at 25ºC. All chemicals were used as received without further purifications.

General Procedures

Synthesis. Synthesis of the model Thy-Thy and its photoproduct Thy<>Thy was performed following the procedure reported in the literature (ref D and F or G), experimental details and NMR spectra are given in the Supporting Information.

Steady-State Photolysis. All irradiations were carried out in a mixture of MeCN:H_2O (1:1, v:v) under oxygen-free conditions at room temperature using 3 mL quartz cuvettes of 1 cm optical path. Monochromatic irradiations (at λ_{exc}= 310 nm) were run using a xenon lamp (150 W) equipped with a monochromator from Photon Technology International (PTI). The course of the photoreaction was followed by HPLC. All irradiated samples were prepared using the same concentration of Thy-Thy (3.5 mM), while the concentration of ForC was fixed at 1 mM and the concentration of ForU (0.38 mM) was adjusted in order to obtain the same absorbance at the irradiation wavelength (λ_{exc} = 310 nm) as that of ForC.

UV-Vis spectrophotometry. The absorption spectra were registered with a single beam spectrophotometer (Cary 50) using a quartz cell of 1 cm optical path.

Phosphorescence Emission. The phosphorescence experiments were performed using ethanol solutions of ForU and ForC, adjusting their absorbance at ca. 0.8 (value determined for a 1 cm optical path) at the excitation wavelength of 280 nm. Solutions were then transferred to quartz tubes of 5 mm diameter. The emission was measured at 77 K, with a gate time of 50 μs, and a delay of 500 μs.

Laser Flash Photolysis. Laser flash photolysis experiments were performed exciting at 266 nm, using the 4th harmonic of a pulsed Nd:YAG laser (L52137V LOTIS TII) with a pulse duration of 6-8 ns. The full system consists in a pulsed laser, a Xenon lamp (Lo 255 Oriel), a monochromator (Oriel 77200), a photomultiplier (Oriel 70705) and an oscilloscope (TDS-640A Tektronic). The output signal from the oscilloscope was transferred to a personal computer. All experiments were performed in a quartz cell of 1 cm optical path length. Concentration of each compound was adjusted in order to have an absorbance of ca. 0.4 at 266 nm. Experiments were carried out in MeCN:H_2O (1:1, v:v) under N_2 atmosphere, solution was renewed after 5 shots in order to avoid degradation of the sample. A laser intensity ranging from 20 to 25 mJ per pulse was used.

The rate constants k_q for TETT reactions were obtained from the Stern–Volmer plots. Briefly, stock solutions of 12 mM Thy-Thy were prepared, so it was only necessary to add microliters to the sample to obtain appropriate quencher concentrations. The bimolecular rate constants, k_q were obtained from the plots by using the following equation:

$$\tau_0/\tau = 1 + k_q\tau_0 \text{ [Thy-Thy]}$$

in which τ_0 is the lifetime of ForU or ForC in the absence of Thy-Thy and τ is the lifetime after the addition of a given quencher concentration [Thy-Thy].

HPLC. All irradiation mixtures were analyzed by HPLC equipped with a diode array detector (DAD), for all chromatograms the detection wavelength was 240 nm. Samples were analyzed using a reverse phase Mediterranea Sea C18 (25 mm Å~ 0.46 mm, 5 μm) column, and the chromatographic conditions were an isocratic mixture of H_2O (at pH 3, adjusted with trifluoroacetic acid): acetonitrile (20:80, v:v) at a flow rate of 1 mL/min. The injection volume was of 10 μL. The photodegradation yields of Thy-Thy were determined from calibration curve using pure samples.

^1H NMR analysis. NMR spectra were recorded on a 300 MHz instrument. Monochromatically irradiated samples (λ_{exc}= 310 nm) of Thy-Thy with ForU or ForC in

MeCN:H_2O (1:1, v:v) under oxygen-free conditions were analyzed by ^{1}H NMR spectroscopy after 1 h irradiation. The samples were dried under reduced pressure and redissolved in CD_3CN:D_2O (1:1, v:v). The signal of HDO was used as reference with a chemical shift of ca. 4.79 ppm. The photodegradation yield of Thy-Thy was determined by comparing the integral of the singlet signal of H6 protons in Thy-Thy at δ 7.75 ppm and Thy<>Thy at δ 4.35 ppm, same analysis was run with protons of methyl group at N3 (δ 3.71 and 3.47 ppm, respectively) and at C5 (δ 2.25 and 1.80 ppm, respectively).

Computational details. Geometry optimizations on a π-stacked ForC-Thy model system (Figure S1) were conducted using the density functional theory (DFT) method for the ground state (S_0) and its time-dependent extension (TD-DFT) for the excited states (S_1 and T_1), making use of the dispersion-corrected hybrid DFT/ωB97-XD functional and the Pople 6-31+G** basis set, as implemented in the Gaussian 09 program.[1] The Tamm-Dancoff approximation was used for all TD-DFT computations.[2] Note that all the calculations have been performed in gas-phase. As a general comment, while the performance of the ωB97-XD exchange-correlation functional has been benchmarked against *ab initio* CASPT2 computations in our previous work,[3] the role of dispersion is crucial since we are dealing with stacked dimers for which geometries obtained by non-dispersion corrected functionals are largely inaccurate. This can be seen as a supplementary argument in favor of the use of the ωB97-XD functional that natively includes dispersion corrections. Finally, no conformational study has been performed since the dimer has been built in such a way to reproduce the orientation of the two chromophores in a B-DNA disposition.

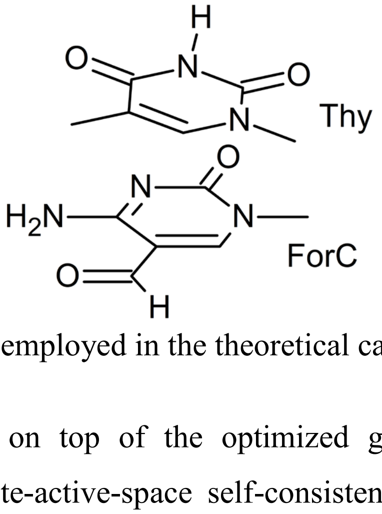

Figure S1. ForC-Thy model employed in the theoretical calculations.

Energies were recomputed on top of the optimized geometries by means of the multiconfigurational complete-active-space self-consistent field/complete-active-space second-order perturbation theory (CASSCF/CASPT2) method and the ANO-S-VDZP as implemented in the OpenMolcas software.[4] The CASSCF wave functions were built distributing 14 electrons into 13 molecular orbitals [hereafter, CAS(14,13)]. The orbitals are displayed in Figure S2. The active space is composed by the three most important π and π* orbitals localized over each molecule, *i.e.* six p-like molecular orbitals of ForC and 6 of Thy, and the lone pair on the oxygen of the aldehyde group of ForC. This extension of the widely used CAS(12,12) for DNA nucleobase dimers[5–9] plus the mentioned lone pair, to allow n,π* transitions, is chemically intuitive and has been proved as accurate in the ForU-Thy system.[10] Twelve singlet states and twelve triplet states were computed in the state-average (SA)-CASSCF procedures.

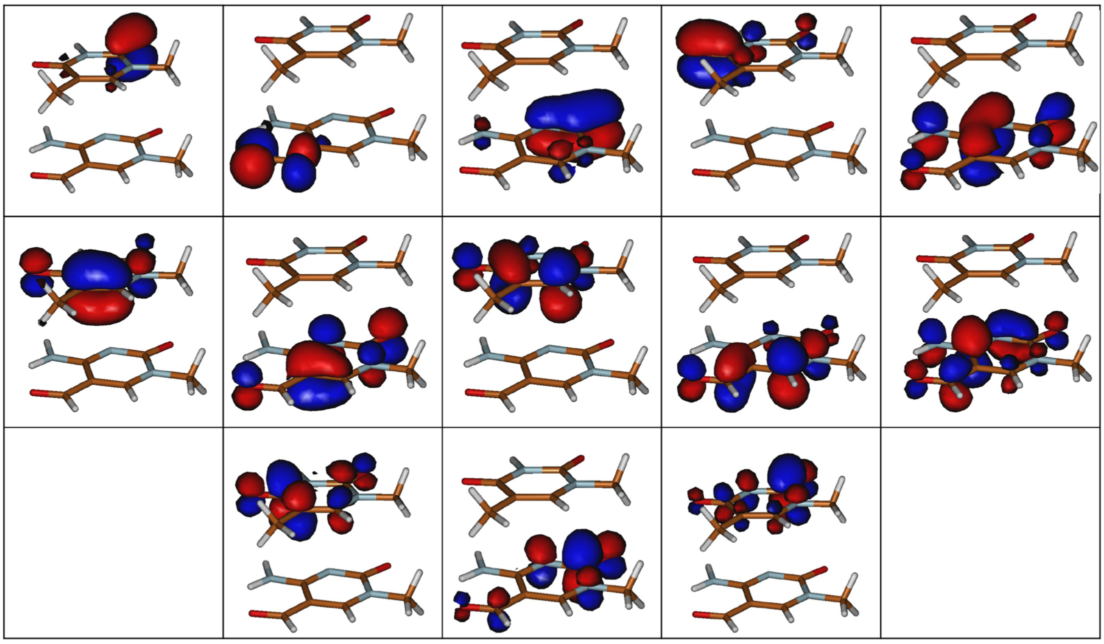

Figure S2. CASSCF orbitals corresponding to the CAS(14,13) active space.

The necessary electron dynamic correlation has been computed at the CASPT2 level using the CAS(14,13) wave functions as a reference. The original zeroth-order Hamiltonian has been used throughout (IPEA=0.0 au), whereas an imaginary level shift of 0.2 au has been used to avoid the presence of weakly intruder states.

Synthetic details and characterization of Thy-Thy and Thy<>Thy

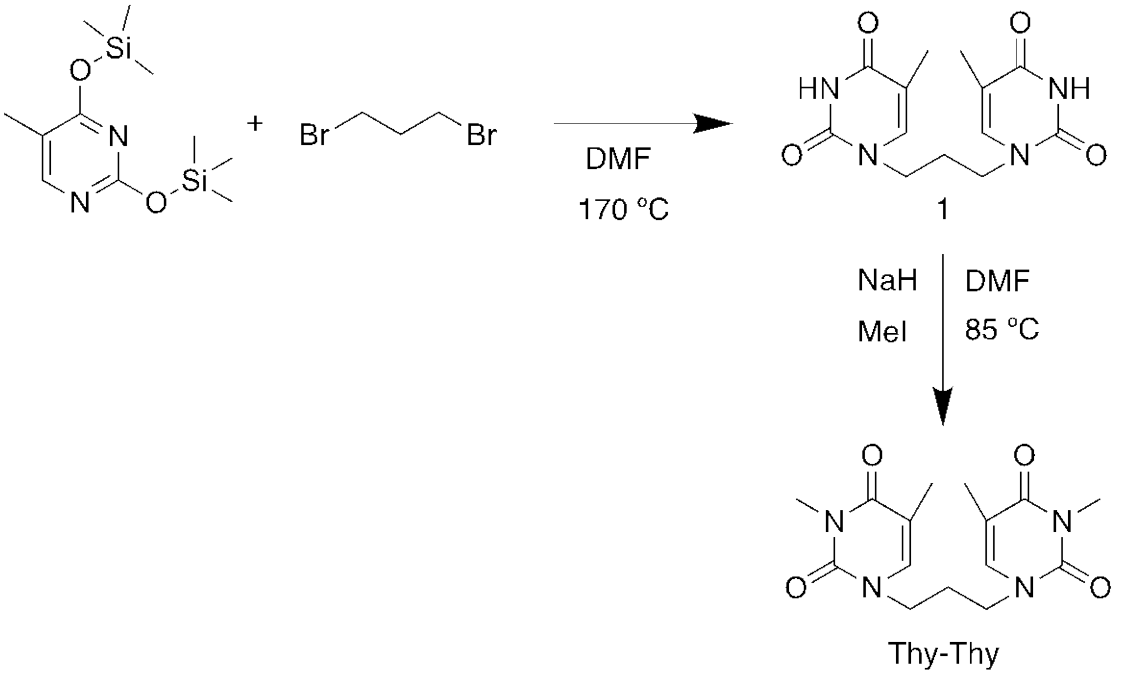

Scheme S1. Synthesis of methylated thymine dimer (Thy-Thy)

Synthesis of 1,1'-(propane-1,3-diyl)bis(5-methylpyrimidine-2,4(1H,3H)-dione) (1). To a dry deaerated two necks round bottom flask fitted with a reflux condenser was added o,o'-bis(trimethylsilyl)thymine (1 g, 3.7 mmol) and 6 mL of anhydrous dimethylformamide. Then, 1,3-dibromopropane (0.19 mL, 1.8 mmol) was added and the solution was stirred at 170 ºC overnight. The resulting mixture was cooled to 0 ºC and 3 mL of methanol were added to obtain a white precipitate, that was washed with a mixture of chloroform:methanol (1:1, v:v) and dried under vacuum. Finally, the pure product **1** was obtained as a white solid and used as reaction intermediate without further purification. Yield: 0.420 g (77%). ^{1}H NMR (300 MHz, DMSO-d_6): δ (ppm) 11.21 (s, 2H), 7.52 (s, 2H), 3.65 (t, J = 6.9 Hz, 4H), 1.92-1.87 (m, 2H), 1.74 (s, 6H).

Synthesis of 1,1'-(propane-1,3-diyl)bis(3,5-dimethylpyrimidine-2,4(1H,3H)-dione) (Thy-Thy). Compound **1** (0.395 g, 1.34 mmol), NaH (0.07 g, 2.94 mmol) and 9 mL of anhydrous dimethylformamide were added to a dry two necks round bottom flask fitted with a reflux condenser. This mixture was stirred at room temperature for 1h. Subsequently, the solution was cooled in an ice bath and then methyl iodide (MeI, 0.462

mL, 7.42 mmol) was added portionwise. The resulting mixture was stirred at 85 ºC overnight. Finally, the crude reaction was concentrated under reduced pressure and purified by column chromatography (CH_2Cl_2:MeOH, 99:1) to give the pure product Thy-Thy. Yield: 0.264 g (61%). ^{1}H NMR (300 MHz, $CDCl_3$): δ (ppm) 7.05 (s, 2H), 3.78 (t, *J* = 6.9 Hz, 4H), 3.33 (s, 6H), 2.13-2.04 (m, 2H), 1.92 (s, 6H).^{13}C NMR (75 MHz, $CDCl_3$) δ ppm: 163.8 (2CO), 151.8 (2CO), 137.9 (2CH), 110.3 (2C), 46.8 ($2CH_2$), 28.7 (CH_2), 28.1 ($2CH_3$), 13.1 ($2CH_3$).

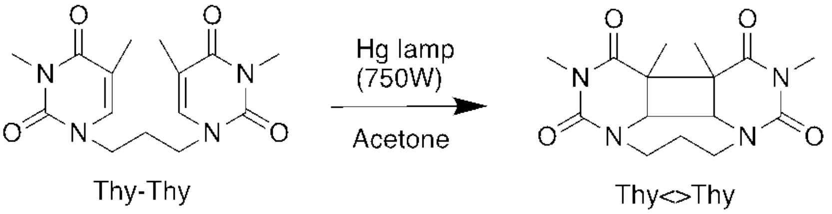

Scheme S2. Synthesis of cyclobutane dimer of Thy-Thy (Thy<>Thy)

Synthesis of 5,6a,6b,8-tetramethylhexahydro-1H-3a,5,8,9a-tetraazacyclohepta[def]biphenylene-4,6,7,9(5H,8H)-tetraone (Thy<>Thy).

0.02 g (0.034 mmol) of compound **2** was dissolved in acetone (30 mL). This solution was split up among three pyrex tubes which were irradiated with a medium pressure mercury lamp (750 W). The solvent was evaporated to give the pure product **3**. Yield 0.02 g (> 98 %). ^{1}H NMR (300 MHz, $CDCl_3$) δ ppm: 4.44 (m, 1H), 4.39 (m, 1H), 3.75 (s, 2H), 3.11 (s, 6H), 2.68 (m, 2H), 2.29 (m, 1H), 1.61 (m, 1H), 1.56 (s, 6H). ^{13}C NMR (75 MHz, $CDCl_3$) δ ppm: 169.0 (2CO), 151.5 (2CO), 60.0 (2CH), 49.1 ($2CH_2$), 46.0 (2C), 28.2 ($2CH_3$), 23.9 (CH_2), 21.3 ($2CH_3$).

Supplementary Figures S3-S8

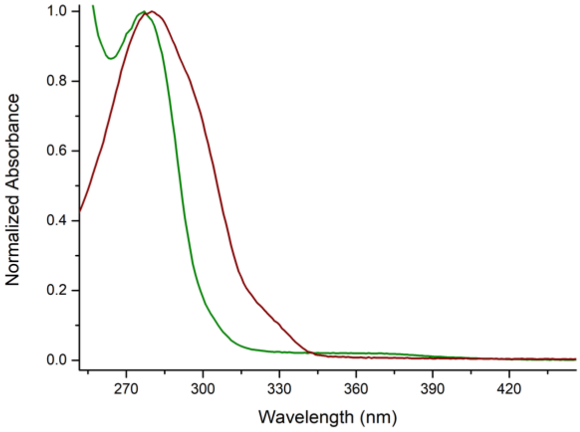

Figure S3. Normalized UV-vis absorption spectra of 5-formyluracil (ForU, red) and 5-formylcytosine (ForC, green) in MeCN:H_2O (1:1, v:v).

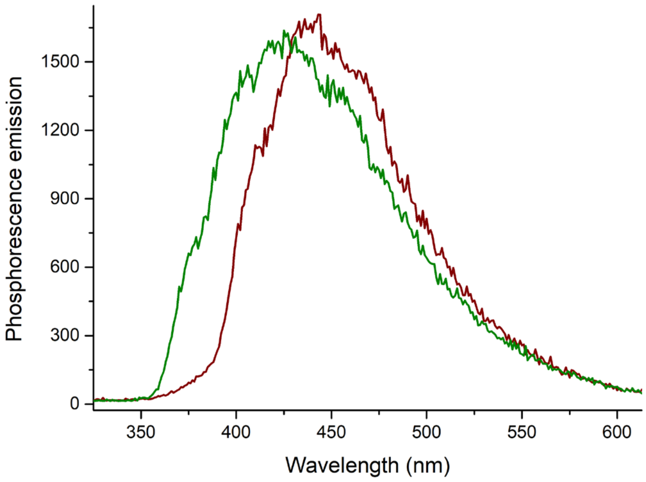

Figure S4. Phosphorescence emission spectra of 5-formyluracil (ForU, red) and 5-formylcytosine (ForC, green) in EtOH at 77 K (λ_{exc} = 280 nm).

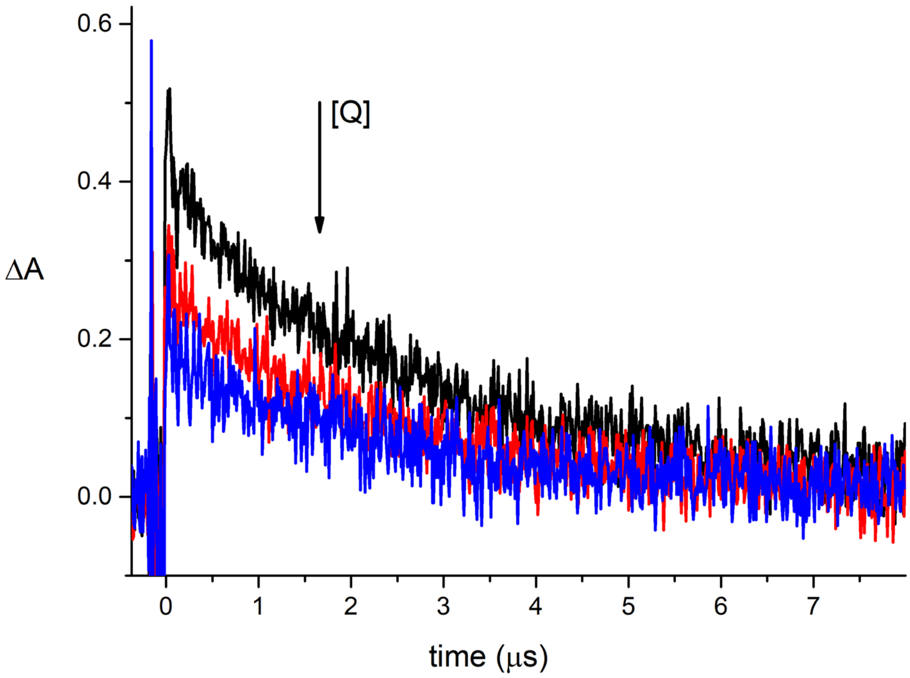

Figure S5. Decays of ForC in deaerated MeCN:H_2O (1:1,v:v) at 440 nm after the laser pulse at 266 nm in the presence of different Thy-Thy concentrations (from 0 to 0.08 mM).

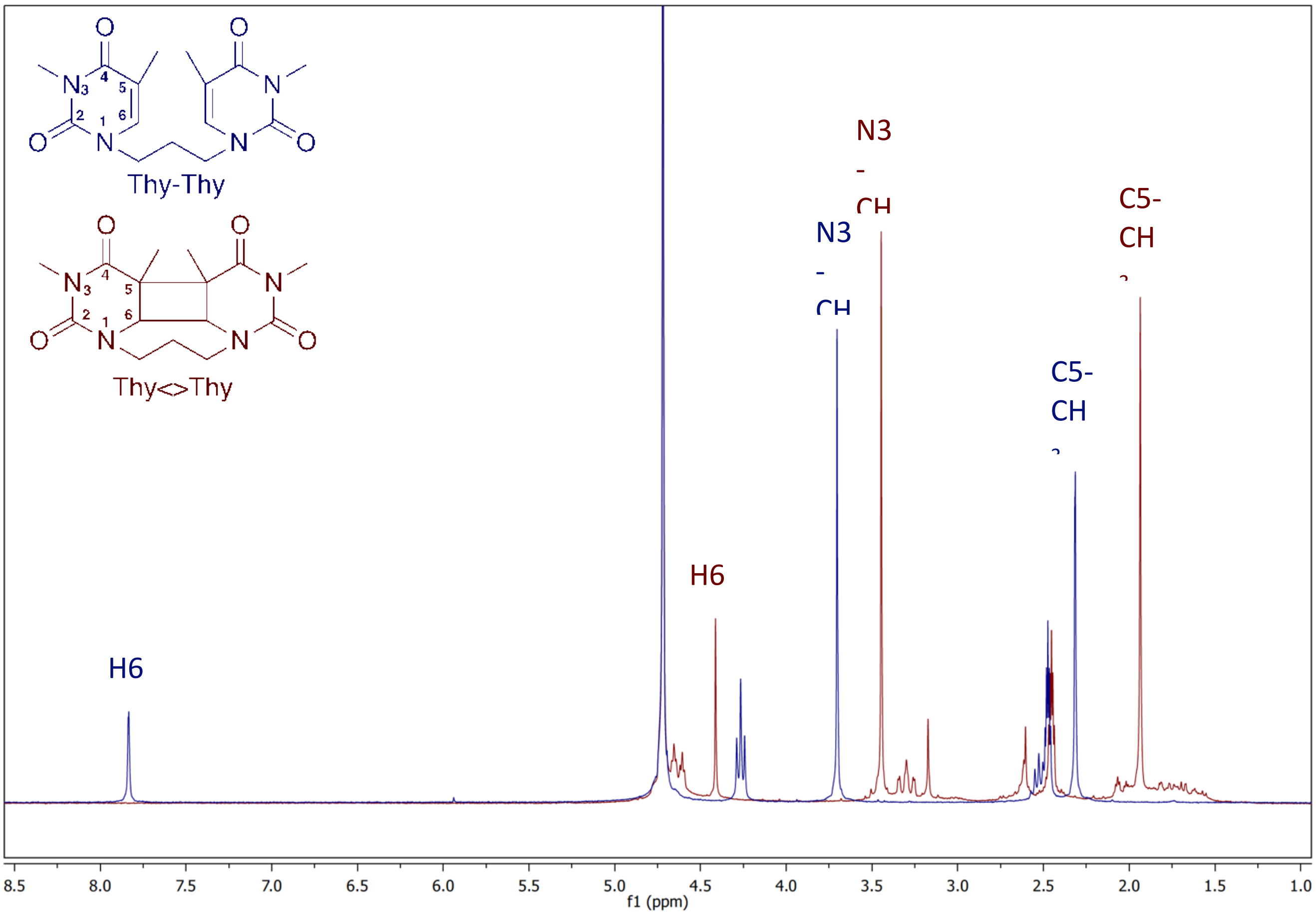

Figure S6. ^{1}H NMR (D_2O:CD_3CN, v:v, 300 MHz) of pure Thy-Thy (blue line) and Thy<>Thy (red line)

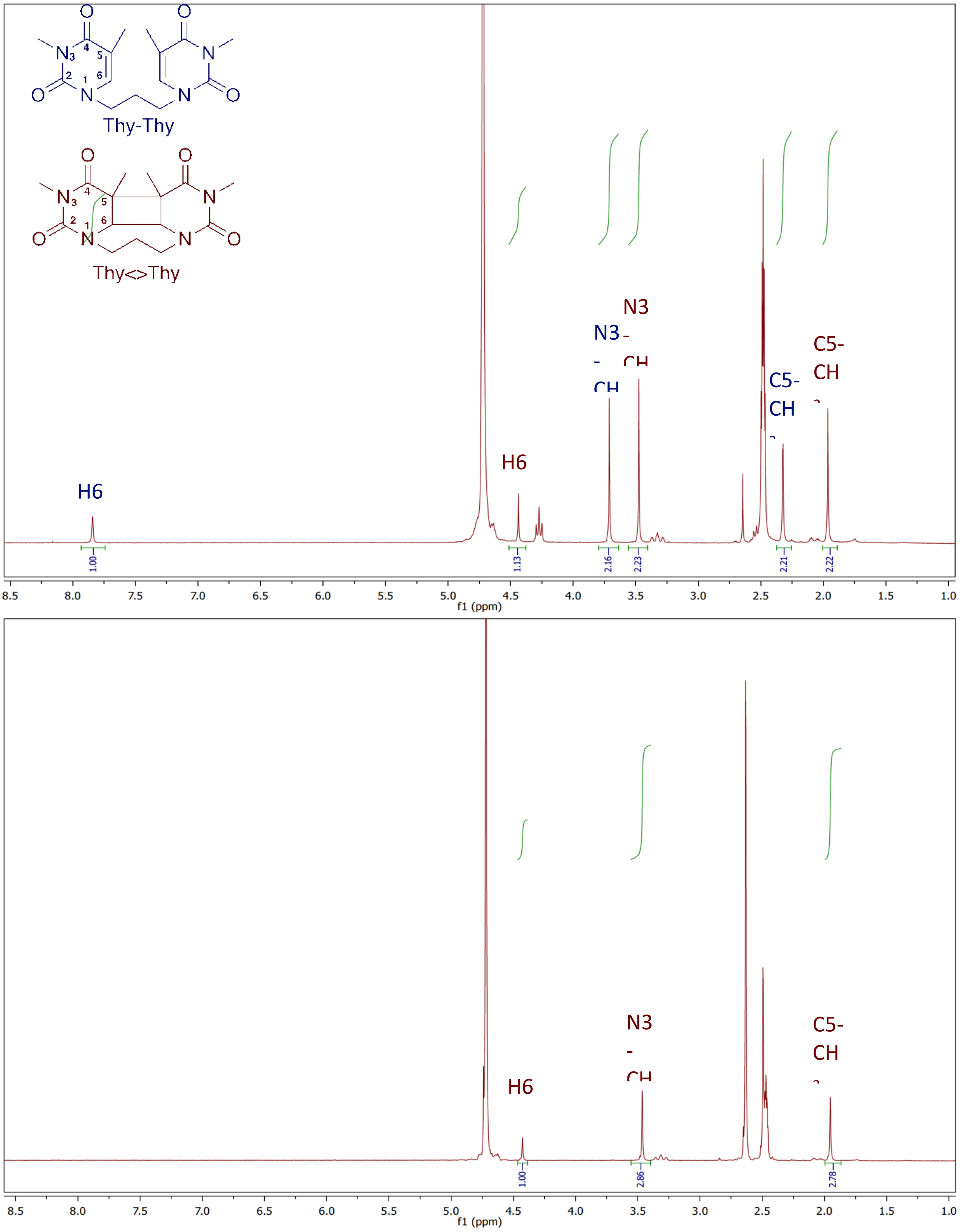

Figure S7. ^{1}H NMR spectrum in D_2O/CD_3CN (1:1, v:v) of the 60 min irradiation at 310 nm of ForC:Thy-Thy (1 mM:3.5 mM, top) and ForU:Thy-Thy (0.38 mM:3.5 mM, bottom).

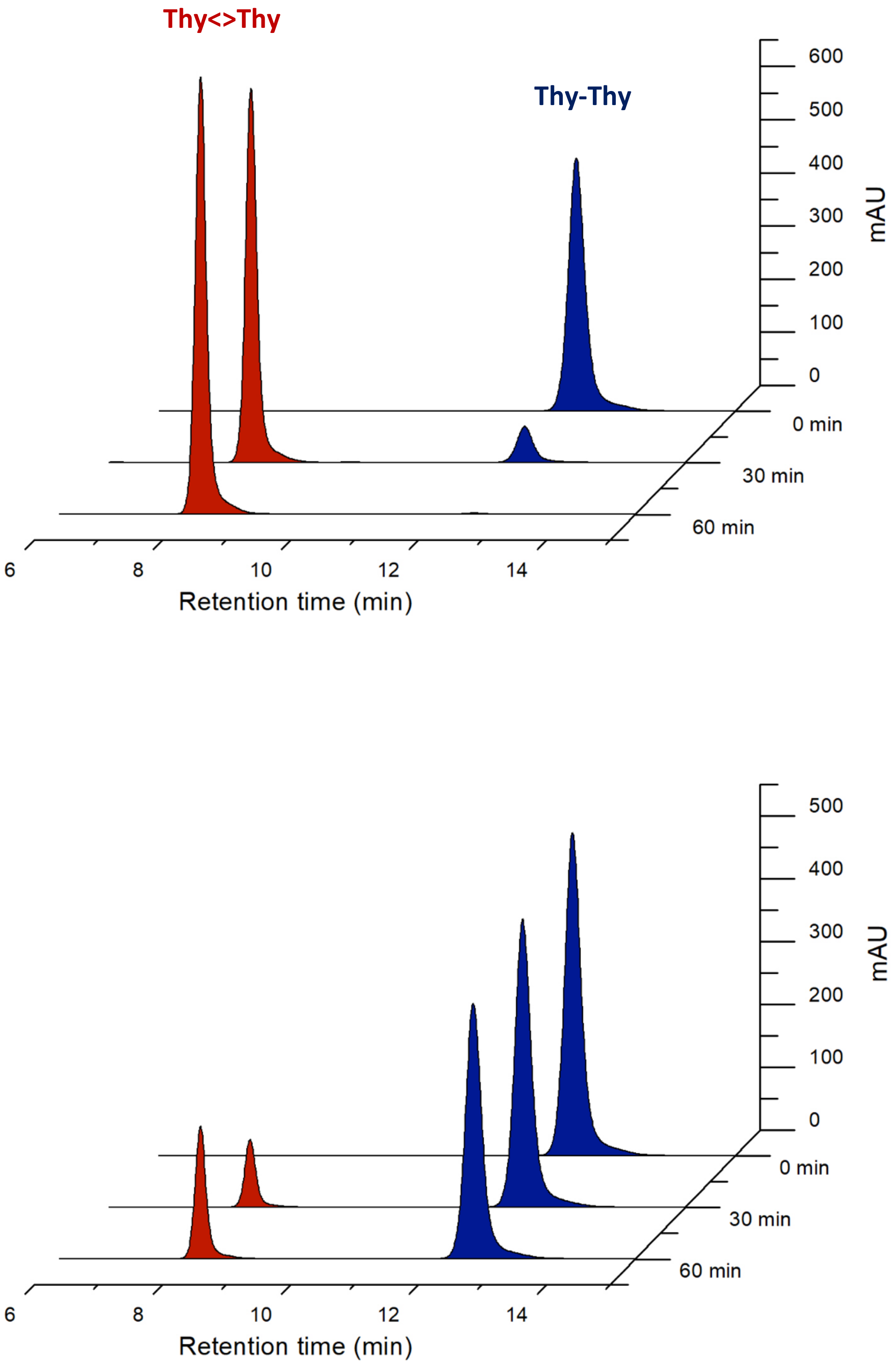

Figure S8. HPLC chromatograms registered at 240 nm for monochromatic irradiation (λ_{exc}= 310 nm) from 0 to 60 min of Thy-Thy (3.5 mM) in H_2O:MeCN (1:1, v:v) alone (bottom) or in the presence of ForU (0.38 mM, up)

ForC-Thy spin-orbit couplings

Spin-orbit-couplings (SOCs) between the most relevant singlet and triplet states of the ForC-Thy system were computed by means of the restricted-active-space state interaction method[11,12] using the atomic mean field approximation,[13,14] as described in detail elsewhere.[15,16] The SOC values were computed between twelve singlet and twelve triplet states, and the results are summarized in Table S1.

Table S1. SOC values (in cm^{-1}) between the most relevant singlet and triplet states of ForC-Thy. The nature f the states is shown in Figure 9 of the main text.

	^{3}EXC$_1$	**^{3}EXC$_2$**	**^{3}(n,π*)$_{\mathrm{ForC}}$**
		S$_0$ min	
^{1}(n,π*)$_{\mathrm{ForC}}$	6.6–18.9	5.6–16.1	~0.1
^{1}(π,π*)$_{\mathrm{ForC}}$	0.1	0.1	2.1–5.0
^{1}(π,π*)$_{\mathrm{Thy}}$	0.1	0.1	0.5–1.4
		^{1}(n,π*)$_{\mathrm{ForC}}$ min	
^{1}(n,π*)$_{\mathrm{ForC}}$	14.7–42.8[a]	0.2–0.7[b]	2.9–7.9
^{1}(π,π*)$_{\mathrm{ForC}}$	1.8–3.4	0.0	3.3–9.1
^{1}(π,π*)$_{\mathrm{Thy}}$	0.2–0.5	0.0–0.1	1.0–2.8
		^{3}EXC$_1$ min	
^{1}(n,π*)$_{\mathrm{ForC}}$	4.2–11.1	10.0–26.1	1.0–2.4
^{1}(π,π*)$_{\mathrm{ForC}}$	0.3–0.4	0.4–1.5	0.1–0.3
^{1}(π,π*)$_{\mathrm{Thy}}$	1.6–4.2	4.4–11.4	2.5–6.3

[a] At this ^{1}(n,π*)$_{\mathrm{ForC}}$ min geometry, the first triplet state can be labelled as ^{3}(π,π*)$_{\mathrm{ForC}}$. The relatively high SOC value with the ^{1}(n,p*)$_{\mathrm{ForC}}$ state is coherent with this fact.

[b] At this ^{1}(n,π*)$_{\mathrm{ForC}}$ min geometry, the second triplet state can be labelled as ^{3}(π,π*)$_{\mathrm{Thy}}$. The low SOC value with the ^{1}(n,p*)$_{\mathrm{ForC}}$ state is coherent with this fact.

References

(1) M. J. Frisch, G.; Trucks, W.; Schlegel, H. B.; Scuseria, G. E.; Robb, M. A.; Cheeseman, J. R.; Scalmani, G.; Barone, V.; Mennucci, B.; Petersson, G. A.; et al. Gaussian 09, Revision D.01. *Inc.: Wallingford, CT*. 2009.

(2) Hirata, S.; Head-Gordon, M. Time-Dependent Density Functional Theory within the Tamm–Dancoff Approximation. *Chem. Phys. Lett.* **1999**, *314* (3), 291–299.

(3) Francés-Monerris, A.; Lineros-Rosa, M.; Miranda, M. A.; Lhiaubet-Vallet, V.; Monari, A. Photoinduced Intersystem Crossing in DNA Oxidative Lesions and Epigenetic Intermediates. *Chem. Commun.* **2020**, *56* (32), 4404–4407.

(4) Fdez. Galván, I.; Vacher, M.; Alavi, A.; Angeli, C.; Aquilante, F.; Autschbach, J.; Bao, J. J.; Bokarev, S. I.; Bogdanov, N. A.; Carlson, R. K.; et al. OpenMolcas: From Source Code to Insight. *J. Chem. Theory Comput.* **2019**, *15* (11), doi: 10.1021/acs.jctc.9b00532.

(5) Gonzalez-Ramirez, I.; Roca-Sanjuan, D.; Climent, T.; Serrano-Perez, J. J.; Merchan, M.; Serrano-Andres, L. On the Photoproduction of DNA/RNA Cyclobutane Pyrimidine Dimers. *Theor. Chem. Acc.* **2011**, *128* (4–6), 705–711.

(6) Serrano-Pérez, J. J.; González-Ramírez, I.; Coto, P. B.; Merchán, M.; Serrano-Andrés, L. Theoretical Insight into the Intrinsic Ultrafast Formation of Cyclobutane Pyrimidine Dimers in UV-Irradiated DNA: Thymine versus Cytosine. *J. Phys. Chem. B* **2008**, *112* (45), 14096–14098.

(7) Olaso-Gonzalez, G.; Roca-Sanjuan, D.; Serrano-Andres, L.; Merchan, M. Toward the Understanding of DNA Fluorescence: The Singlet Excimer of Cytosine. *J. Chem. Phys.* **2006**, *125*, 231102.

(8) Climent, T.; González-Ramírez, I.; González-Luque, R.; Merchán, M.; Serrano-Andrés, L. Cyclobutane Pyrimidine Photodimerization of DNA/RNA Nucleobases in the Triplet State. *J. Phys. Chem. Lett.* **2010**, *1* (14), 2072–2076.

(9) Roca-Sanjuan, D.; Olaso-Gonzalez, G.; Gonzalez-Ramirez, I.; Serrano-Andres, L.; Merchan, M. Molecular Basis of DNA Photodimerization: Intrinsic Production of Cyclobutane Cytosine Dimers. *J. Am. Chem. Soc.* **2008**, *130* (32), 10768–10779.

(10) Francés-Monerris, A.; Hognon, C.; Miranda, M. A.; Lhiaubet-Vallet, V.; Monari, A. Triplet Photosensitization Mechanism of Thymine by an Oxidized Nucleobase: From a Dimeric Model to DNA Environment. *Phys. Chem. Chem. Phys.* **2018**, *20* (40), 25666–25675.

(11) Malmqvist, P. A.; Roos, B. O.; Schimmelpfennig, B. The Restricted Active Space (RAS) State Interaction Approach with Spin-Orbit Coupling. *Chem. Phys. Lett.* **2002**, *357* (3–4), 230–240.

(12) Roos, B. O.; Malmqvist, P. Å. Relativistic Quantum Chemistry: The Multiconfigurational Approach. *Phys. Chem. Chem. Phys.* **2004**, *6* (11), 2919–2927.

(13) Hess, B. A.; Marian, C. M.; Wahlgren, U.; Gropen, O. A Mean-Field Spin-Orbit Method Applicable to Correlated Wavefunctions. *Chem. Phys. Lett.* **1996**, *251* (5–6), 365–371.

(14) Christiansen, O.; Gauss, J.; Schimmelpfennig, B. Spin-Orbit Coupling Constants from Coupled-Cluster Response Theory. *Phys. Chem. Chem. Phys.* **2000**, *2* (5), 965–971.

(15) Frances-Monerris, A.; Segarra-Marti, J.; Merchan, M.; Roca-Sanjuan, D. Theoretical Study on the Excited-State Pi-Stacking versus Intermolecular Hydrogen-Transfer Processes in the Guanine-Cytosine/Cytosine Trimer. *Theor. Chem. Acc.* **2016**, *135* (2), 31.

(16) Londesborough, M. G. S.; Dolansky, J.; Jelinek, T.; Kennedy, J. D.; Cisarova, I.; Kennedy, R. D.; Roca-Sanjuan, D.; Frances-Monerris, A.; Lang, K.; Clegg, W. Substitution of the Laser Borane Anti-B18H22 with Pyridine: A Structural and Photophysical Study of Some Unusually Structured Macropolyhedral Boron Hydrides. *Dalt. Trans.* **2018**, *47*, 1709–1725.

Cartesian coordinates of the ForC-Thy model

S_0 min (DFT/ωB97-XD)

C	-1.702520	0.048007	3.251852
N	-1.237171	-0.591934	2.023773
C	-0.903761	-1.983375	2.091830
O	-1.026522	-2.538788	3.177089
N	-0.469999	-2.598091	0.964989
C	-0.378328	-1.929893	-0.176569
N	0.059261	-2.577079	-1.258917
C	-0.734396	-0.531589	-0.287876
C	-1.155544	0.073734	0.869215
H	-0.916418	0.017442	4.007318
H	-1.434706	1.123129	0.888926
C	-0.657405	0.248436	-1.507098
H	0.382435	-3.528410	-1.167784
H	0.168016	-2.071420	-2.129331
C	1.868285	-1.212637	4.144233
N	2.262252	-1.634855	2.803080
C	2.516168	-2.979961	2.620953
O	2.432466	-3.800865	3.520103
N	2.893085	-3.316483	1.337327
C	3.015086	-2.479301	0.231656
O	3.347072	-2.935817	-0.855063
C	2.718022	-1.080503	0.506266
C	2.808208	-0.098941	-0.621915
C	2.361419	-0.740651	1.763188
H	0.921439	-1.684857	4.413936
H	2.126389	0.285625	2.024468
H	3.829627	-0.040048	-1.012665
H	2.503885	0.899787	-0.297678
H	2.161881	-0.404431	-1.450965
H	3.078801	-4.300086	1.184217
H	-0.975716	1.302619	-1.406027
H	-1.960313	1.083740	3.033076
H	-2.578411	-0.480126	3.629954
H	1.754087	-0.128636	4.147947
H	2.636056	-1.496901	4.865960
O	-0.273459	-0.171821	-2.592610

$^1(n,\pi^*)_{\mathrm{ForC}}$ min (TD-DFT/ωB97-XD)

C	-1.580272	0.159343	3.253775
N	-1.161380	-0.569737	2.058926
C	-1.002094	-1.955357	2.155652
O	-1.221247	-2.513111	3.237146
N	-0.572954	-2.629802	1.051427
C	-0.415077	-2.017026	-0.105526
N	0.048550	-2.741962	-1.141809
C	-0.729647	-0.611433	-0.287170
C	-1.061784	0.068361	0.862829
H	-0.929464	-0.100455	4.087667
H	-1.270619	1.130705	0.862005
C	-0.672556	0.033352	-1.559689
H	0.309488	-3.700603	-0.963555
H	0.439560	-2.305210	-1.962525
C	1.816194	-1.330429	4.131696
N	2.205909	-1.668363	2.763147

C	2.474188	-2.991279	2.490706
O	2.386672	-3.877446	3.332606
N	2.865794	-3.243403	1.193546
C	3.013763	-2.327413	0.159660
O	3.390495	-2.705619	-0.948216
C	2.687170	-0.955872	0.513585
C	2.795502	0.109250	-0.535209
C	2.306928	-0.705277	1.786712
H	0.884466	-1.838932	4.386424
H	2.052780	0.298153	2.109946
H	3.830984	0.225163	-0.869847
H	2.444765	1.068866	-0.149001
H	2.196848	-0.145403	-1.415049
H	3.071477	-4.211886	0.980307
H	-0.794421	1.123713	-1.632829
H	-1.510307	1.228107	3.056635
H	-2.607946	-0.101501	3.514708
H	1.676383	-0.252164	4.192654
H	2.600654	-1.632398	4.827005
O	-0.529531	-0.567912	-2.701483

^{3}EXC$_1$ min (TD-DFT/ωB97-XD)

C	-1.399087	0.103665	3.268975
N	-1.068750	-0.759504	2.136865
C	-1.234610	-2.160335	2.289891
O	-1.594935	-2.579240	3.389825
N	-0.993119	-2.968321	1.225208
C	-0.611927	-2.460840	0.059542
N	-0.417444	-3.294454	-0.963997
C	-0.390243	-1.041638	-0.127503
C	-0.617028	-0.242110	0.983368
H	-0.915918	-0.267924	4.171424
H	-0.533691	0.837719	0.928364
C	-0.013608	-0.430296	-1.383351
H	-0.561712	-4.282985	-0.827299
H	-0.129931	-2.922472	-1.861118
C	1.772287	-1.243420	4.016108
N	2.004132	-1.437626	2.586698
C	2.165953	-2.749838	2.157216
O	2.064733	-3.693561	2.925804
N	2.441285	-2.920654	0.818779
C	2.742525	-1.911926	-0.107832
O	3.123310	-2.222700	-1.241743
C	2.572311	-0.571929	0.373273
C	3.002070	0.591378	-0.434712
C	2.084029	-0.357101	1.735560
H	0.906063	-1.826948	4.333963
H	2.124225	0.622806	2.190675
H	3.986024	0.936330	-0.084392
H	2.316642	1.435549	-0.309349
H	3.087842	0.329402	-1.489726
H	2.552117	-3.877526	0.511149
H	0.117820	0.665737	-1.348354
H	-1.049383	1.112182	3.052216
H	-2.478907	0.112133	3.427334
H	1.590302	-0.185018	4.193181
H	2.646638	-1.562457	4.586388
O	0.149254	-1.031059	-2.445573